A comparison of reflection coefficients in porous media from 2D plane-wave analysis & spectral element forward modeling

Haorui Peng, Yanadet Sripanich, Ivan Vasconcelos, Jeannot Trampert

Earth Science Department,Utrecht University

Utrecht University

Summary

The Biot theory provides a general framework for describing the seismic response of porous media. Proper boundary conditions must be specified for the following three cases: the elastic-poroelastic interface, the acoustic-poroelastic interface and the poroelastic-poroelastic interface for accurate modeling and inversion of seismic data. In this study, we first review the expressions for reflection coefficients for all three cases from plane-wave analysis. We subsequently benchmark the first two cases against spectral element method (SEM) forward modeling to verify and ensure consistency between finite-frequency wavelets. We show with numerical examples, that both methods lead to comparable results within frequency range between 5Hz and 80Hz, which is of relevance to exploration seismology.

Porous medium open-pore interface condition

According to Deresiewicz and Skalak (1963), the 2D open-pore interface conditions for acoustic-poroelastic, elastic-poroelastic media are summarized in Table 1. The subscripts z and x indicate the directions of vectors perpendicular and parallel to the interface. The superscript b denotes the bottom poroelastic medium and t denotes the top acoustic or elastic medium in each case, separately. In porous media, $\sigma_{zz}, \sigma_{xz}, \dot{u}_z, \dot{u}_x, \dot{U}_z$ are the stress, velocity fields in the solid frame and the velocity in the fluid part, respectively. ϕ and $\dot{w}_z$ are porosity and the relative velocity of the fluid to the solid frame. In acoustic media, p, $\dot{U}_z$, K_f are the pressure, velocity and the bulk modulus. In the elastic media, $\sigma_{zz}, \sigma_{xz}, \dot{u}_z$ and $\dot{u}_x$ are the stress and velocity, respectively. Expressions of parameters P, Q, R are as follows (Feng and Johnson, 1983):

$$P = \frac{(1-\phi)(1-\phi-\kappa_{fr}/\kappa_s)\kappa_s + \phi(\kappa_s/\kappa_f)\kappa_{fr}}{1-\phi-\kappa_{fr}/\kappa_s + \phi\kappa_s/\kappa_f} + \frac{4N}{3}$$

$$Q = \frac{(1-\phi)(1-\phi-\kappa_{fr}/\kappa_s)\phi\kappa_s}{1-\phi-\kappa_{fr}/\kappa_s + \phi\kappa_s/\kappa_f}$$

$$R = \frac{\phi^2\kappa_s}{1-\phi-\kappa_{fr}/\kappa_s + \phi\kappa_s/\kappa_f}$$

where N is the shear modulus of both drained porous solid and the composite. The pressure drop across the interface requires

$$p^t - p^b = k\dot{w}_z$$

Here k is a coefficient of resistance. The open-pore condition corresponds to $k = 0$ and sealed-pore condition $k = \infty$ (i.e. $\dot{w}_z = 0$ and p^t and p^b are not related). In this research we will focus on the open-pore condition. As can be seen from Table 1, the number of equations for the interface condition varies with that of the physical parameters from 4 to 5, which yield relations for reflection/transmission (R/T) coefficients in two cases.

	acoustic-poroelastic	elastic-poroelastic
interface conditions	$-p^t = \sigma^b_{zz} - \phi^b p^b$ $\sigma^t_{zx} = 0$ $p^t = p^b$ $\dot{U}^t_z = (1-\phi^b)\dot{u}^b_z + \dot{U}^b_z$	$\sigma^t_{zz} - \phi^t p^t = \sigma^b_{zz} - \phi^b p^b$ $\sigma^t_{xz} = \sigma^b_{xz}$ $\dot{u}^t_z = \dot{u}^b_z$ $\dot{u}^t_x = \dot{u}^b_x$ $\dot{U}^b_z = \dot{u}^b_z$
physical implications	pressure continuity fluid volume conservation normal stress continuity shear stress disappearance	elastic and solid vertical velocity continuity elastic and solid horizontal velocity continuity solid and fluid vertical velocity continuity normal stress continuity shear stress continuity
constitutive relations	$K^t_f(\nabla\cdot\vec{U}^t) = (P^b - 2N^b + Q^b)\frac{\partial u^b_x}{\partial x}$ $+(P^b + Q^b)\frac{\partial u^b_z}{\partial z} + (Q^b + R^b)(\nabla\cdot\vec{U}^b)$ $(\frac{\partial u^t_z}{\partial x} + \frac{\partial u^t_x}{\partial z}) = 0$ $K^t_f(\nabla\cdot\vec{U}^t) = (Q^b(\nabla\cdot\vec{u}^b) + R^b(\nabla\cdot\vec{U}^b))/\phi^b$ $U^t_z = \phi U^b_z + (1-\phi^b)u^b_z$	$\lambda^t\frac{\partial u^t_x}{\partial x} + (\lambda^t + 2\mu^t)\frac{\partial u^t_z}{\partial z} =$ $(P^b - 2N^b + Q^b)\frac{\partial u^b_x}{\partial x} + (P^b + Q^b)\frac{\partial u^b_z}{\partial z}$ $+(Q^b + R^b)(\nabla\cdot\vec{U}^b)$ $\mu^t(\frac{\partial u^t_z}{\partial x} + \frac{\partial u^t_x}{\partial z}) = N^b(\frac{\partial u^b_z}{\partial x} + \frac{\partial u^b_x}{\partial z})$ $u^t_z = u^b_z$ $u^t_x = u^b_x$ $U^b_z = u^b_z$

Table 1: Comparison of different porous media interface conditions

The R/T coefficients equations for an acoustic-poroelastic interface are available in Wu et al., (1990) while the other cases can be derived in a similar way. Solving the specified systems of equations will give the corresponding R/T coefficients.

Acoustic-poroelastic modeling

An explosive source (yellow star) is placed horizontally in the middle of the two-layer model and 6 λ above the interface, where λ is the P wavelength in the acoustic medium above the interface. A line of receivers (in black) is placed at the same height as the source with horizontal positions decided by the P wave incidence angles, from 0 degree to 1 degree below the critical angle. The source time function is a Ricker wavelet with the peak frequency of 15Hz. We use the same material parameters as in Wu's paper (Table 2) with a critical angle of 35 degrees.

Acoustic layer
Density $\rho = 1000\ kg/m^3$ P wave velocity $C_p = 1500\ m/s$
Poroelastic layer
Solid density $\rho_s = 2480\ kg/m^3$ Fluid density $\rho_f = 1000\ kg/m^3$ Porosity $\phi = 0.38$ Tortuosity $c = 1.79$ Solid bulk modulus $\kappa_s = 49.9\ GPa$ Fluid bulk modulus $\kappa_f = 2.25\ GPa$ Frame bulk modulus $\kappa_{fr} = 5.17\ GPa$ Fluid viscosity $\eta_f = 0\ Pa\cdot s$ Frame shear modulus $\mu_{fr} = 2.80\ GPa$ Fast P wave velocity $C_{p1} = 2657\ m/s$ Slow P wave velocity $C_{p2} = 935\ m/s$ S wave velocity $C_s = 1281\ m/s$

Table 2: Acoustic-poroelastic parameters

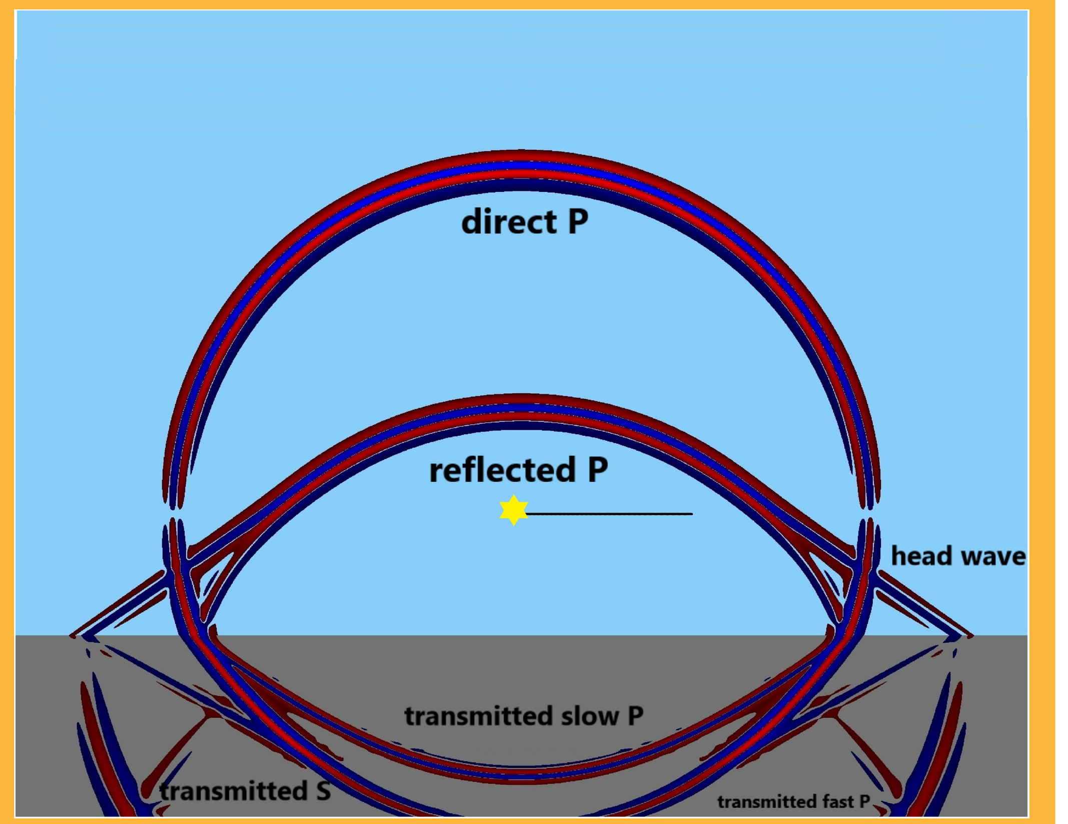

Figure 3: Wavefield snapshot of acoustic-poroelastic interface SEM forward modeling

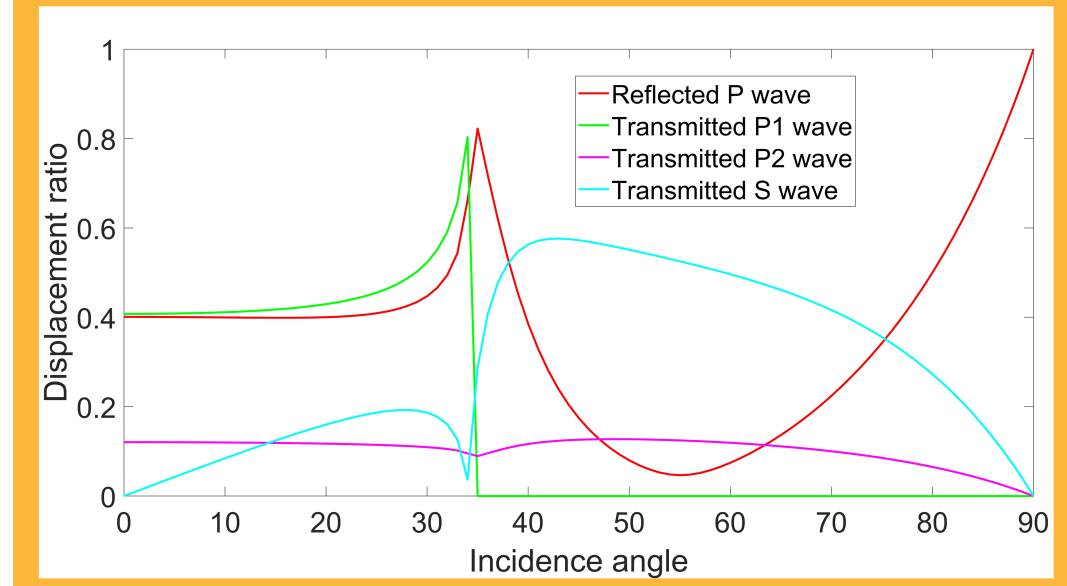

Figure 1: Absolute R/T coefficients of displacement for acoustic-poroelastic interface as a function of incidence angle

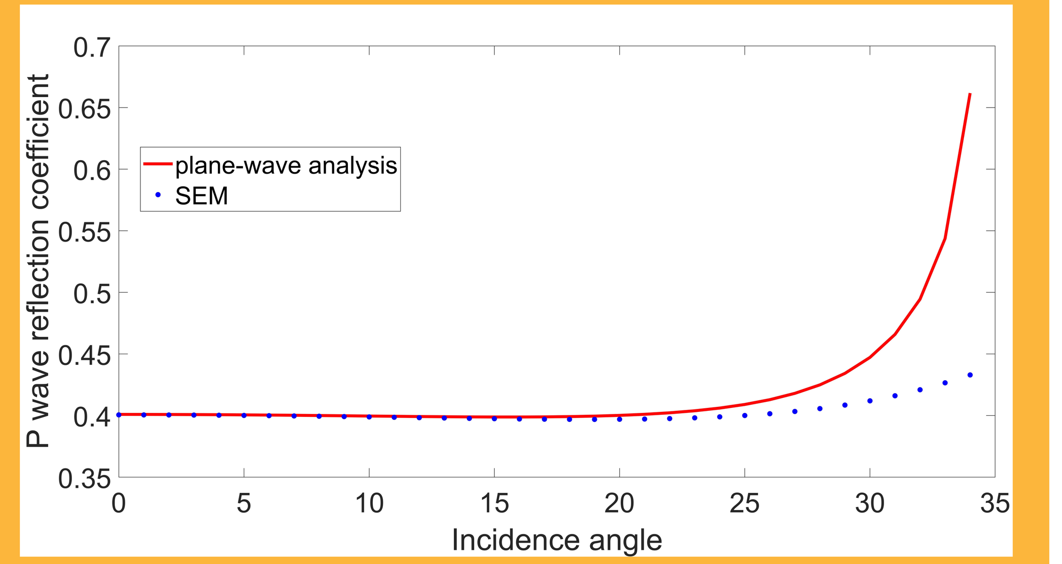

Figure 4: Comparison of absolute P wave reflection coefficient for acoustic-poroelastic interface

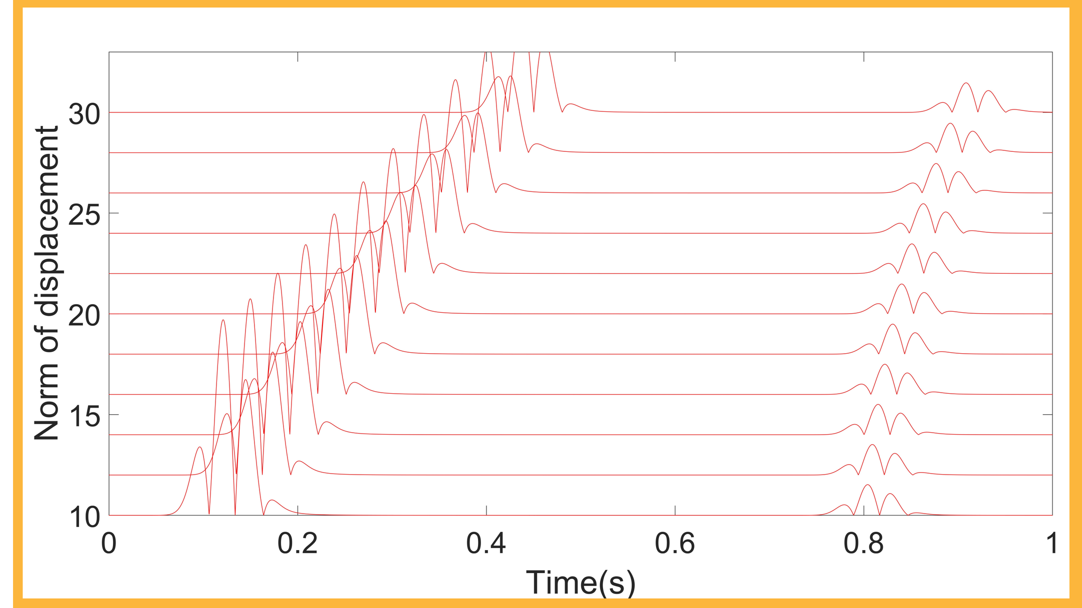

Figure 2: Norm of displacement for receiver 10 to 30

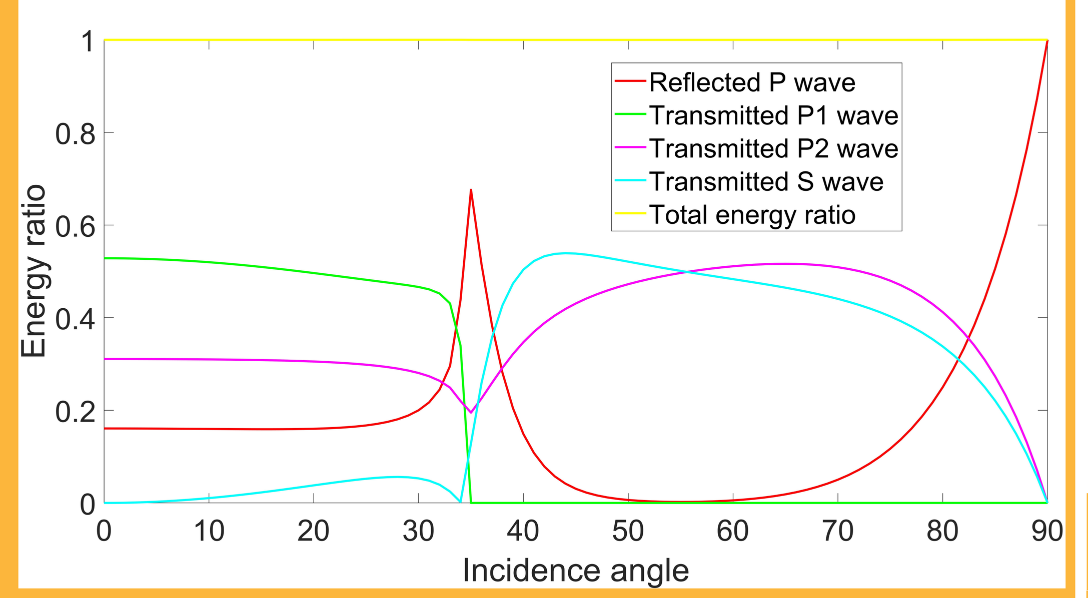

Figure 5: Energy ratio as a function of incidence angle

Elastic-poroelastic modeling

The geometric system is similar to the previous case. The material parameters listed in Table 3 are from Morency (2008) with a critical angle of 55 degrees. We run simulations for a series of peak Ricker frequencies (5Hz, 15Hz, 40Hz, 60Hz, and 80Hz) to study frequency-dependent effects.

Elastic layer
Density $\rho = 2650\ kg/m^3$ P wave velocity $C_p = 2219\ m/s$ S wave veolocity $C_s = 1325\ m/s$
Poroelastic layer
Solid density $\rho_s = 2200\ kg/m^3$ Fluid density $\rho_f = 950\ kg/m^3$ Porosity $\phi = 0.4$ Tortuosity $c = 2$ Permeability $k = 10^{-9}m^2$ Solid bulk modulus $\kappa_s = 6.9\ GPa$ Fluid bulk modulus $\kappa_f = 2.0\ GPa$ Frame bulk modulus $\kappa_{fr} = 6.7\ GPa$ Fluid viscosity $\eta_f = 0.001\ Pa\cdot s$ Frame shear modulus $\mu_{fr} = 3.0\ GPa$ Fast P wave velocity $C_{p1} = 2693\ m/s$ Slow P wave velocity $C_{p2} = 1186\ m/s$ S wave velocity $C_s = 1410\ m/s$

Table 3: Elastic-poroelastic parameters

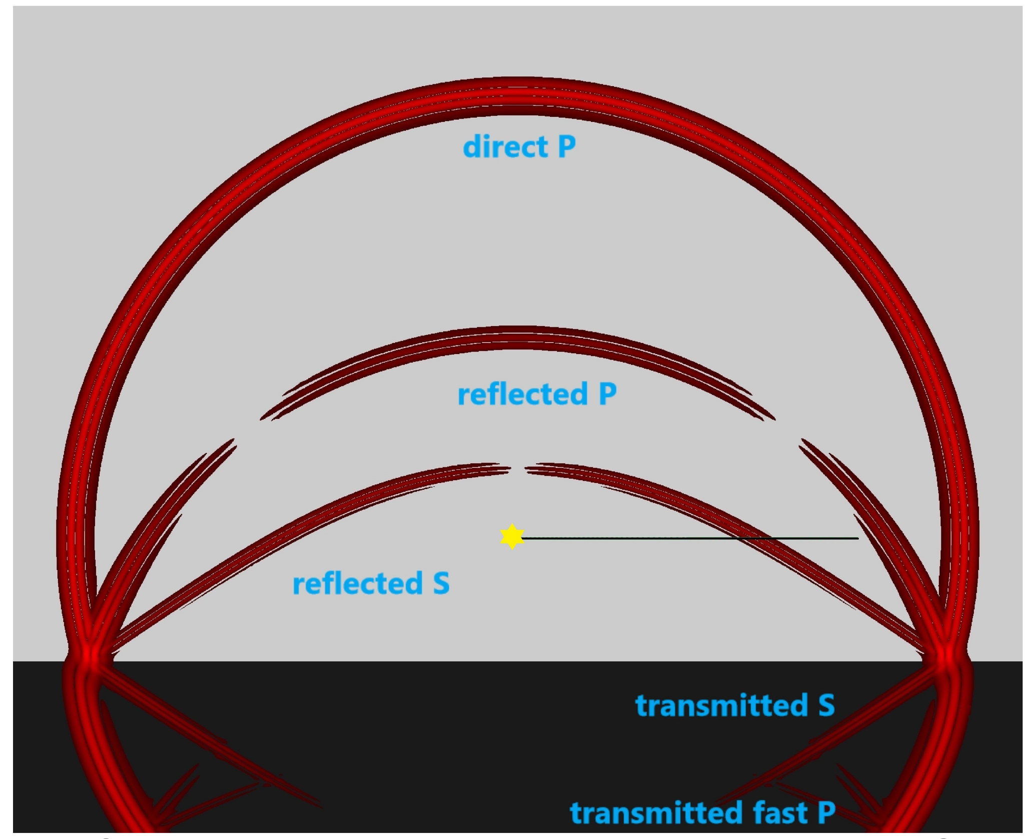

Figure 8: Wavefield snapshot of elastic-poroelastic interface SEM forward modeling

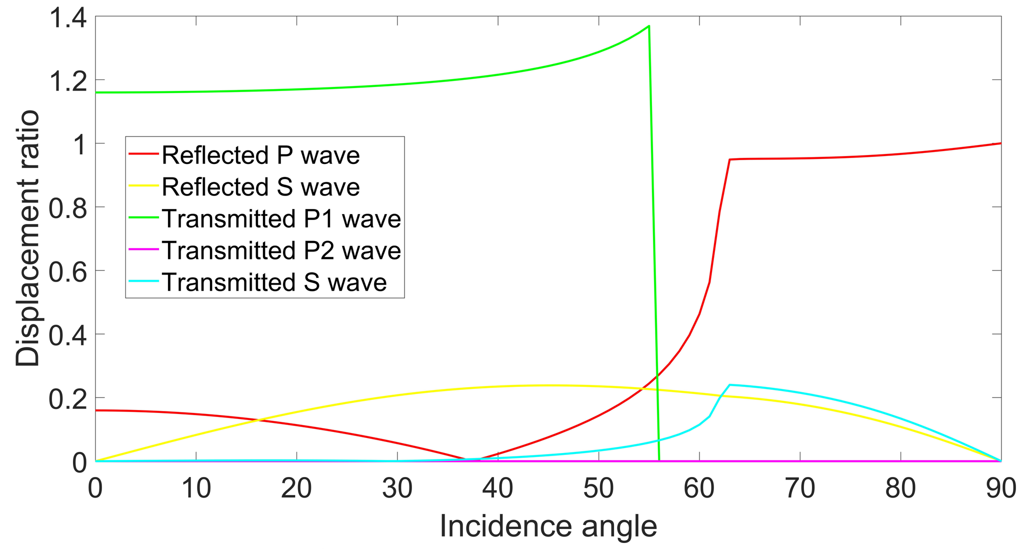

Figure 6: Absolute R/T coefficients of displacement for elastic-poroelastic interface as a function of incidence angle

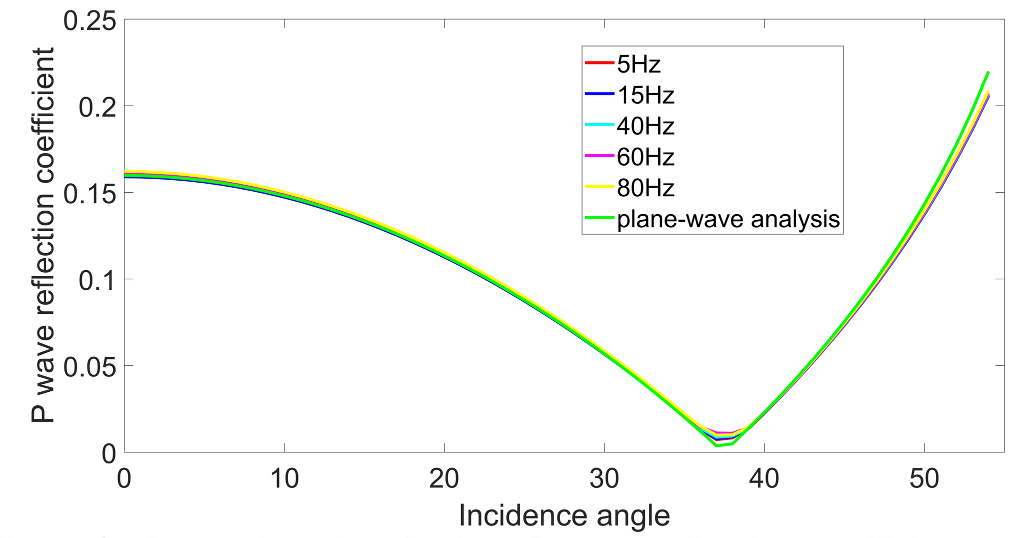

Figure 9: Comparison for absolute P wave reflection coefficients between different frequencies for elastic-poroelastic interface

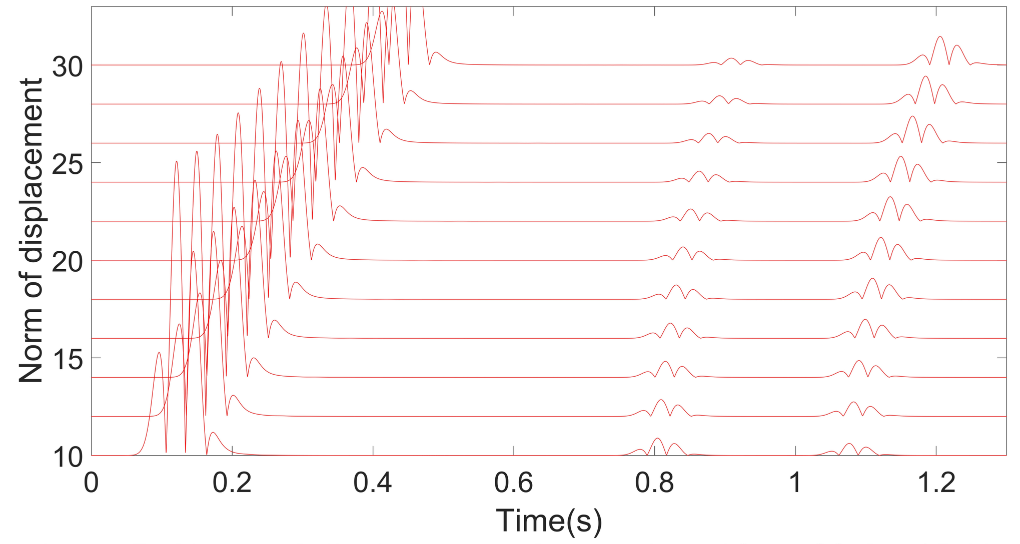

Figure 7: Norm of displacement for receiver 10 to 30 for 15 Hz

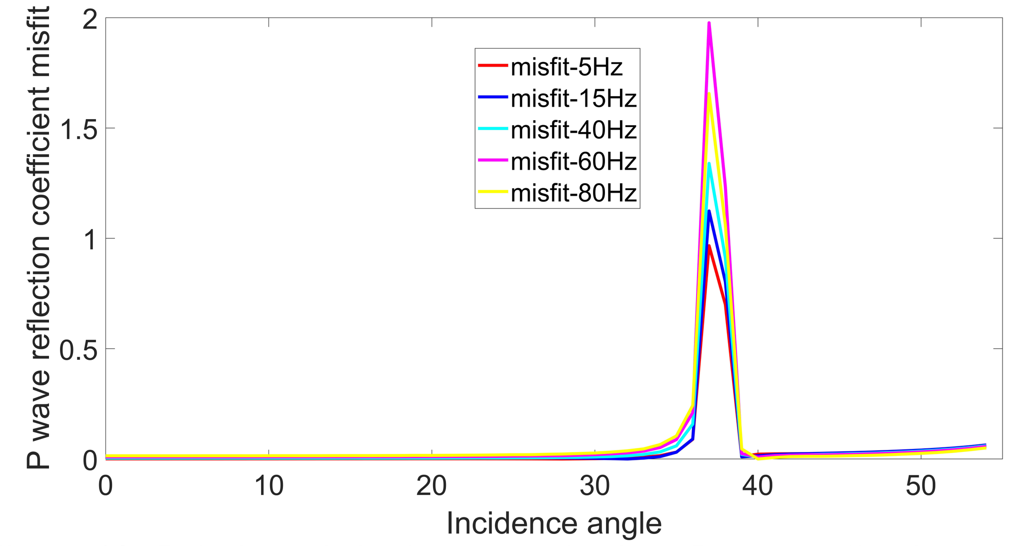

Figure 10: Relative misfits between absolute P wave reflection coefficients as a function of incidence angle

Bibliography

Feng, S., and D. L. Johnson, 1983, High-frequency acoustic properties of a fluid/porous solid interface. I. New surface mode: The Journal of the Acoustical Society of America, 74, 906.

Morency, C., Y. Luo, and J. Tromp, 2011, Acoustic, elastic and poroelastic simulations of CO_2 sequestration crosswell monitoring based on spectral-element and adjoint methods: Geophysical Journal International, 185, 955–966.

Deresiewicz, H., and R. Skalak, 1963, On uniqueness in dynamic poroelasticity: Bulletin of the Seismological Society of America, 53, 783–788.

Wu, Q. X., and L. Adler, 1990, Reflection and transmission of elastic waves from a fluid-saturated porous solid boundary: The Journal of the Acoustical Society of America, 87, 2349.